CONF-970726--2
WAPD-T--3114

THE INITIATION OF ENVIRONMENTALLY-ASSISTED CRACKING IN SEMI-ELLIPTICAL SURFACE CRACKS

L. A. James

U.S. Department of Energy Contract DE-AC11-93PN38195

Proposed for Submittal to the
1997 ASME Pressure Vessel and Piping Conference

BETTIS ATOMIC POWER LABORATORY PITTSBURGH, PENNSYLVANIA 15122-0079

Operated for the U.S. Department of Energy
by WESTINGHOUSE ELECTRIC CORPORATION

DISCLAIMER

THE INITIATION OF ENVIRONMENTALLY-ASSISTED CRACKING IN SEMI-ELLIPTICAL SURFACE CRACKS

Lee A. James*
Advisory Engineer

Bettis Atomic Power Laboratory
Westinghouse Electric Corporation
West Mifflin, PA 15122-0079

ABSTRACT

A criterion to predict under what conditions EAC would initiate in cracks in a high-sulfur steel in contact with low-oxygen water was recently proposed by Wire and Li. This EAC Initiation Criterion was developed using transient analyses for the diffusion of sulfides plus experimental test results. The experiments were conducted mainly on compact tension-type specimens with initial crack depths of about 2.54 mm. The present paper expands upon the work of Wire and Li by presenting results for significantly deeper initial semi-elliptical surface cracks. In addition, in one specimen, the surface crack penetrated weld-deposited cladding into the high-sulfur steel. The results for the semi-elliptical surface cracks agreed quite well with the EAC Initiation Criterion, and provide confirmation of the applicability of the criterion to crack configurations with more restricted access to water.

INTRODUCTION

Following the pioneering work of Kondo et al. (Kondo, 1972a, 1972b), a phenomenon generally known as environmentally-assisted cracking (EAC) has received a great deal of attention in the nuclear industry worldwide because it has the potential to cause significant in-service crack extension. The EAC phenomenon can occur in low-alloy steels (e.g., ASTM A302-B, A533-B, A508-2) in elevated temperature aqueous environments typical of those found in commercial boiling-water reactors (BWR) or pressurized-water reactors (PWR). The occurrence, or non-occurrence, of EAC is dependent upon the attainment of a "critical" concentration of hydrogen sulfide at the crack tip; probably of the order of 2-5 ppm (VanDerSluys and Emanuelson, 1993). The instantaneous sulfide concentration at the crack tip is the net balance between the competing processes of sulfide supply and sulfide loss. In lieu of water-borne sulfur contamination, the only source of sulfides to the crack tip is the growing crack itself, which intersects metallurgical sulfide inclusions (MnS, FeS, etc.) embedded within the steel. These inclusions then dissolve in the aqueous crack-tip environment and supply sulfide ions to the crack tip. Sulfides can be removed from the crack-tip region by any one, or more, of four mass-transport processes: 1) diffusion due to a sulfide ion concentration gradient from the crack tip to the crack mouth (e.g., Turnbull 1982, 1992; Wire, 1996), 2) ion migration due to an electrochemical corrosion potential (ECP) gradient from the crack tip to the crack mouth (e.g., Turnbull, 1982), 3) fatigue "pumping" or advection due to cyclic motion of the crack walls (e.g., Hartt, 1978; Turnbull, 1983), and 4) convective transport induced within the crack enclave by an external (to the crack) stream flow (e.g., James 1995a, 1996a). Not all of these mass-transport processes play a significant role in every

---

*Fellow ASME

case of corrosion-fatigue crack growth. For example, the second process, ion migration, is probably an important factor in the case of oxygenated BWR environments, where a significant ECP gradient can exist between the crack tip and the crack mouth. Potential gradients between the crack tip and crack mouth are much smaller for low-oxygen PWR environments (Gabetta, 1987). The third mass-transport process, fatigue "pumping" is likely to be a factor only at relatively high cyclic frequencies, and the fourth process, convective mass transport, would not be an important consideration under quasi-stagnant flow conditions. Note, however, that the first mass-transport process, diffusion, would be operative any time that a concentration gradient exists between the crack tip and the crack mouth. In fact, diffusion was essentially the only mass-transport operative in the experiments to be described herein because they were conducted in low-oxygen water at low cyclic frequencies under quasi-stagnant flow conditions.

EAC initiates when the concentration of hydrogen sulfide at the crack tip reaches a "critical" level, which is the net result of the competing processes of sulfide supply and sulfide loss. If a crack tip is initially free of sulfides (i.e., H_2S < 2-5 ppm), the crack must extend into the steel at an average rate (or velocity, $\bar{V}$) that is sufficient to raise the sulfide concentration to the critical level. In this context, the average crack velocity is defined as the crack extension (Δa) for some increment of time, divided by the total time associated with that increment (i.e., load rise-time plus load fall-time plus all dwell periods between or during fatigue cycles). The product of the average crack velocity and the average sulfur content of the steel is proportional to the rate of sulfide supply. Atkinson and Forest (1985) qualitatively identified the role of crack tip velocity in the supply rate of sulfide ions, and stated that a "critical" crack velocity was needed to cause EAC in several cases. Combrade et al. (1988) presented a quantitative approach whereby the steady-state sulfide concentration at the crack tip would be determined by a balance of sulfide supply by the growing crack and sulfide loss by diffusion. Combrade's steady-state model predicted that, in low-oxygen water at 288°C, EAC would initiate if the crack velocity exceeded a critical value (≈ 10^{-5} mm/sec.), and would also cease if the crack velocity dropped below that same critical value. Wire and Li (1996) coupled transient diffusion calculations with a series of experiments wherein EAC was initiated from cracks in high-sulfur steels which were initially free of sulfide ions. They showed that, in a high-sulfur steel tested in a low-oxygen environment at 243°C, a critical crack velocity ($\bar{V}_{in}$) of approximately 5 x 10^{-7} mm/sec. was required to initiate EAC from an initially clean crack, and that this critical crack velocity had to be maintained for some minimum amount of crack extension (Δa_{crit}) of about 0.33 mm. Most of the experiments of Wire and Li were performed on compact tension (CT) specimens with crack depths (from the notch) of about 2.54 mm. The present study expands upon the work of Wire and Li by employing the same heat of high-sulfur steel and utilizing semi-elliptical surface cracks of considerably greater depths. In one case, the semi-elliptical crack penetrates a monolithic piece of steel, while in the other case the surface crack penetrates weld-deposited cladding and extends into the steel.

EXPERIMENTAL PROCEDURE

The low-alloy steel employed in this study was a high-sulfur ASTM A302-B plate steel (UNS K12022). This heat of steel (Heat 21478-10) has been employed in several previous corrosion-fatigue studies, and readily exhibits EAC when tested under conditions conducive to EAC (e.g., see James 1994a, 1995a, 1997a). The tensile properties and strain-hardening behavior of this heat were described by James (1995b), and the MnS inclusion attributes (specifically, the MnS area fraction) of this heat are given in James and Poskie (1993). As pointed out by Wire and Li (1996), the product of the MnS area fraction and the crack velocity is a better indicator of sulfide ion supply rate than the product of the bulk sulfur content and the crack velocity. The

chemical analysis of the steel is given in Table I. The material was in the quenched and tempered condition (James, 1995b).

The surface-cracked specimen that was employed was described by James and Wilson (1994b). This specimen design features a tight "natural" intersection of the crack and the free surface; i.e., no fatigue starter notches to "short-circuit" the mass-transport path for sulfide ions. The K-solution of Newman and Raju (1984) was employed to calculate the stress intensity factor (K).

Two specimens were tested in this study. One of these specimens (SC-15) was composed of a monolithic piece of the high-sulfur A302-B steel. The other specimen (YJ2CS1) also contained the high-sulfur A302-B steel, but was constructed such that the semi-elliptical surface crack penetrated about 6.1 mm of weld-deposited (gas-metal-arc process) Alloy EN82H (UNS N06082) cladding. Sufficient Alloy 600 (UNS N06600) was then electron beam welded to the Alloy EN82H to allow fabrication of the specimen. The completed weldment assembly was given a post-weld heat-treatment of 607°C for 24 hours. This composite steel/Alloy EN82H/Alloy 600 surface-cracked specimen is similar to those employed in earlier studies (James et al., 1997b, 1997c) and is illustrated in Figure 1.

The water chemistry has been described in several previous publications (James et al., 1994a, 1995a, 1997a, 1997b, 1997c). The concentration of dissolved hydrogen was in the range of 30-40 ml H_2/kg H_2O, and this resulted in low levels of dissolved oxygen (probably $O_2 \leq 10$ ppb). The test temperature was 243°C, and as stated previously, this heat of A302-B has exhibited EAC in this water chemistry numerous times at 243°C.

Since $\bar{V}_{in}$ is the velocity to which a "clean" (i.e., relatively free of sulfides) crack must be driven in order to initiate EAC, it is necessary to start an EAC initiation experiment with a "clean" crack tip. Combrade et al. (1988) pointed out that when a crack growth specimen is precracked in an air environment, a significant number of undissolved metallurgical sulfide inclusions will be present on the exposed crack flanks. These sulfide inclusions begin to dissolve upon the introduction of the aqueous autoclave environment, and hence the specimen may be predisposed toward exhibiting EAC early in the test. Therefore, such sulfide ions must be removed from the crack prior to starting the EAC initiation experiment. This was done by employing high water flow parallel to the crack (e.g., see James et al., 1995a, 1997a, 1997c) to flush the sulfide ions from the crack, and/or by employing an ECP gradient to remove the sulfide ions by ion migration. That these procedures for "cleaning" the crack tip were successful is evidenced by the fact that EAC was not initially observed in these high-sulfur steel specimens.

RESULTS AND DISCUSSION

Monolithic Steel Specimen

As discussed earlier, Specimen SC-15 was composed entirely of the high-sulfur A302-B steel. The crack dimensions at the start of EAC initiation testing were: crack depth a = 13.82 mm, and crack length 2c = 30.48 mm. The test was conducted at a cyclic frequency of 1.67×10^{-3} Hz employing a positive sawtooth waveform (85% load-rise, 15% load-fall) and a stress ratio $R = P_{min}/P_{max} = 0.1$.

The pre-test and post-test crack dimensions were measured on the specimen fracture face which was exposed by fracturing the specimen after soaking in liquid nitrogen at the completion of testing. Figure 2 compares the predicted crack extension behavior with the actual behavior. Crack extension predictions were made on the basis of two different assumptions: mean EAC along the entire surface crack periphery, or mean non-EAC along the entire crack periphery. The mean EAC and non-EAC crack growth relationships for high-sulfur steels in low-oxygen water at 243°C were established by James (1994a) using compact tension (CT) specimens, and good

agreement has been observed between CT specimens and the type of surface-cracked specimens employed herein (e.g., James et al., 1995a, 1997a, 1997b, 1997c). Figure 2 clearly shows that EAC was not observed at the surface of the specimen; the actual crack length is quite close to that predicted for mean non-EAC conditions, while the predicted length would obviously have been much greater by the end of the experiment had EAC been operative.

On the other hand, as seen in Figure 2, the actual crack depth is somewhat greater than that predicted using the mean non-EAC crack growth equations. The end-of-test crack depth is significantly smaller than would have been predicted had mean EAC crack growth rates been operative during the entire experiment, and this suggests at least two possible scenarios: 1) crack growth rates intermediate between mean non-EAC and mean EAC were operative at the deepest point of the crack throughout the entire experiment, or 2) mean non-EAC behavior was operative through the first part of the experiment, after which EAC initiated locally. In order to help resolve the correct scenario, the specimens were fractured in liquid nitrogen following testing, and the local crack extension (Δa_ϕ) was measured around the crack periphery at several values of the elliptical angle (ϕ). The elliptical angle is defined in Figure 3. A photomacrograph of the post-test fracture surface is shown in Figure 4. The in-test crack extension is a narrow band (approximately 0.201-0.503 mm-wide) along the periphery of the crack from ϕ=0° to ϕ=70°. However, it will be observed that over the increment 80° < ϕ < 100°, the in-test crack extension is greater; approximately 1.52 mm. As will be discussed next, it is believed that this larger increment of crack extension at the deepest point of the crack represented the initiation of EAC.

Local crack extensions (Δa_ϕ) were measured at several values of ϕ around the crack periphery and local fatigue crack growth rates (da_ϕ/dN) were calculated for each location. Local values of ΔK (ΔK_ϕ) were also calculated for each location using the Newman and Raju (1984) solution. The Environmental Ratio (ER) is then defined as the observed crack growth rate at a given ϕ (da_ϕ/dN) divided by the crack growth expected in an air environment at that local value of ΔK_ϕ; the equation of Eason et al. (1989) for the mean behavior in air for this class of steels was employed. The ER therefore represents the environmental enhancement in crack growth rates, relative to an air environment, at any locality around the crack periphery.

Because EAC (or non-EAC) is dependent upon the net balance between the competing processes of crack-tip sulfide supply versus removal of sulfides by mass transport, it is clear that the mass-transport path length is an important variable in all of the four mass-transport processes discussed earlier. The mass-transport path length for a semi-elliptical surface crack is given by (sin ϕ)(a), where a is the crack depth at ϕ = 90° (see Figure 3). Figure 5 plots the ER as a function of the mass-transport path length (L). The rationale for employing the mass-transport path length as a variable is as follows: local crack growth rates (da_ϕ/dN) are proportional (although not necessarily linearly) to the local sulfide ion concentration, which in turn is proportional to the mass-transport path length. Figure 5 shows that the ER increases almost linearly from ϕ = 0° to ϕ = 70°, and then increases significantly between ϕ = 70° and ϕ = 90°. Similar measurements of the ER as a function of the mass-transport path length were reported by James (1997d) for cases of steady-state EAC and steady-state non-EAC. It was concluded in that study that the coefficient (C) in the crack growth power law

$$\frac{da}{dN} = C(\Delta K)^n \qquad [1]$$

was not constant for surface cracks in ferritic steels undergoing corrosion-fatigue in high-temperature water; i.e., C was a function of the mass-transport path length:

$$\frac{da_\phi}{dN} = C_\phi(\Delta K_\phi)^n \qquad [2]$$

The present results for $0° \leq \phi \leq 70°$ shown in Figure 5 confirm the earlier observations of James (1997d). Both the absolute values of the ER for $0° \leq \phi \leq 70°$ and the rate of change of the ER (d(ER)/d(L)) over $0° \leq \phi \leq 70°$ suggest that EAC was not observed for $\phi \leq 70°$. Values for ER parameters for the present study plus those for previous studies (James, 1997c, 1997d) on semi-elliptical surface cracks are summarized in Table II. Note that in those cases where EAC was not observed, the mean ER over a significant portion of the crack periphery was generally less than about 3.5, while the mean d(ER)/d(L) was generally less than about 0.25 mm^{-1}. On the other hand, the mean values of the ER and d(ER)/d(L) were significantly higher (often an order of magnitude higher) in those cases where EAC was observed. An example of the EAC response from the earlier study of James (1997d) is given in Figure 6. Hence, it is clear that a state of non-EAC existed in Specimen SC-15 over the crack periphery from $\phi = 0°$ to $\phi = 70°$ for essentially the entire length of the experiment. From Figure 4, it is also clear that the same non-EAC conditions were operative from $\phi = 120°$ to $\phi = 180°$. Additionally, it is clear that EAC had initiated over the range $80° < \phi < 00°$ toward the latter stages of the experiment. Had EAC been operative for a larger period of time, the entire crack front would have become involved in a state of EAC, as observed on Specimen SC-11 (Figure 6).

Therefore, one reasonable scenario for the initiation of EAC in Specimen SC-15 is illustrated in Figure 7. This scenario assumes that mean non-EAC conditions were operative at $\phi = 0°$ over the entire experiment. In addition, it is assumed that mean non-EAC conditions were operative at $\phi = 90°$ until a mean case of EAC initiated at $\phi = 90°$ 1575 cycles into the experiment, and that the mean EAC condition continued until the end of the experiment at N = 2270 cycles. It is clear than many other scenarios could be imagined (e.g., slightly higher than mean non-EAC rates at $\phi = 90°$ earlier in the experiment, followed by slightly lower than mean EAC rates later in the experiment, etc.), but the scenario illustrated in Figure 7 is certainly not unreasonable.

The EAC Initiation Velocity ($\bar{V}_{in}$) proposed by Wire and Li (1996) can be applied to assess the initiation of EAC in Specimen SC-15 at $80° < \phi < 100°$. The value of $\bar{V}_{in} = 5 \times 10^{-7}$ mm/sec. was observed for a crack of depth a = 2.54 mm, and because the crack-tip sulfide concentration should be linearly proportional to the diffusion mass-transport path (i.e., "a"), the general form of the EAC Initiation Velocity is

$$\bar{V}_{in} = (5 \times 10^{-7})(2.54/a) = \frac{1.27 \times 10^{-6}}{a} \qquad [3]$$

where $\bar{V}_{in}$ = mm/sec. and a = mm. This means that the minimum average crack velocity to initiate EAC decreases with increasing crack depth. In addition, the average velocity, $\bar{V}_{in}$, must be maintained for some minimum critical amount of crack extension

$$\Delta a_{crit.} = 0.33 \text{ mm} \qquad [4]$$

before EAC will initiate. 0.33 mm represents the minimum Δa that has been observed when EAC initiated. Wire and Li (1996) have shown several cases where larger amounts of crack extension were necessary to initiate EAC.

Assuming the scenario of Figure 7, the calculated crack depth at $\phi = 90°$ at the point of EAC initiation (N = 1575 cycles) is

a = 13.97 mm, and employing Equation [3], the EAC Initiation Velocity should be

$$\bar{V}_{in} = \frac{1.27 \times 10^{-6}}{13.97} = 9.09 \times 10^{-8} \frac{mm}{second}$$

The mean crack velocity ($\bar{V}$) in the test up to N = 1575 cycles, assuming that mean non-EAC conditions prevailed, would be $\bar{V} = 1.57 \times 10^{-7}$ mm/second. Hence, the inequality

$$\bar{V} = 1.57 \times 10^{-7} > 9.09 \times 10^{-8} = \bar{V}_{in}$$

holds and EAC should have initiated provided that Equation [4] is also satisfied. The calculated crack extension at $\phi = 90°$ up to N = 1575 cycles was about 1 mm. Hence, the second inequality

$$\Delta a = 1.0 > 0.33 = \Delta a_{crit}$$

also holds and EAC would be predicted to initiate at $\phi = 90°$. This is, of course, the observed result.

Clad Steel Specimen

The specimen employed in this experiment (Specimen YJ2CS1) is illustrated in Figure 1. The steel portion of the specimen was composed of the same heat of high-sulfur A302-B steel (Heat 21478-10) as Specimens SC-11 and SC-15 described earlier. The crack dimensions at the start of EAC initiation testing were: a = 15.78 mm and 2c = 30.28 mm. 45418 fatigue cycles were applied at R = 0.7 employing a sawtooth loading waveform at 0.0075 Hz. Figure 8 shows the post-test fracture surface. Figure 9 compares the observed and predicted crack dimensions. Crack extension at the surface ($\phi = 0°$) was calculated using the mean relationship from James and Mills (1995c) for weld-deposited Alloy EN82H in low-oxygen water at 243°C. The comparison of actual and predicted crack dimensions in Figure 9 suggests that EAC did not initiate at $\phi = 90°$ during the experiment. The actual crack extension at $\phi = 90°$ was 0.528 mm, and this produced an average crack velocity $\bar{V} = 8.72 \times 10^{-8}$ mm/second. The criterion of Equation [3] would predict that the EAC Initiation Velocity was

$$\bar{V}_{in} = \frac{1.27 \times 10^{-6}}{15.78} = 8.05 \times 10^{-8} \frac{mm}{sec.}$$

Therefore, both parts of the criterion

$$\bar{V} = 8.72 \times 10^{-8} > 8.05 \times 10^{-8} = \bar{V}_{in}$$
$$\Delta a = 0.528 > 0.33 = \Delta a_{crit}$$

would suggest that EAC should have initiated. Note, however, that Equation [3] represents the minimum crack velocity to initiate EAC. Wire and Li (1996) observed several cases where EAC initiated at higher crack velocities in high-sulfur A302-B steels. Therefore, the fact that $\bar{V}$ exceeded $\bar{V}_{in}$ by 8.3-percent and yet EAC had not initiated is not inconsistent with the notion that Equation [3] represents a minimum EAC initiation velocity. It is also clear that the complicating factor of the weld-deposited cladding did not invalidate the EAC Initiation Criterion.

Measurements of the local Δa_ϕ were made on Specimen YJ2CS1, and the resulting ER is plotted as a function of L in Figure 10. The magnitude of the observed ERs, and the rate of change $d(ER)/d(L) = 0.084$ mm^{-1} (for $30° \leq \phi \leq 90°$) again show that EAC did not initiate in Specimen YJ2CS1.

The experiment on Specimen YJ2CS1 also provided the opportunity to compare the observed crack growth behavior in the Alloy EN82H at $\phi = 0°$ with results on wrought Alloy 600 tested under similar conditions by James and Mills (1995c). This comparison is shown in Figure 11, and it will be noted that the agreement is quite good.

SUMMARY AND CONCLUSIONS

The EAC Initiation Criterion proposed by Wire and Li (1996) was developed mainly employing compact tension-type specimens which generally had initial crack depths of about 2.54 mm.

The present paper describes two experiments that were conducted using a more prototypic semi-elliptical surface crack design employing considerably deeper cracks. In addition, one of the experiments featured a semi-elliptical surface crack penetrating weld-deposited cladding into the high sulfur ferritic steel. The two experiments provided an excellent corroboration of the EAC Initiation Criterion: in one case, EAC initiated when the average crack velocity exceeded the minimum initiation velocity by a factor of 1.73, while in the other case EAC did not initiate when the average crack velocity exceeded the minimum initiation velocity by a factor of 1.08. These results should provide additional confidence in the EAC Initiation Criterion proposed by Wire and Li.

ACKNOWLEDGEMENTS

This work was performed under a U.S. Department of Energy contract with the Bettis Atomic Power Laboratory, a unit of Westinghouse Electric Corporation. The efforts of a colleague, Y. Y. Li, in coordinating the difficult fabrication of the clad Specimen YJ2CS1 are appreciated. The experimental portion of this study was conducted under subcontract at Materials Engineering Associates (MEA), Lanham, MD. The efforts of Dr. W. H. Cullen of MEA in contributing to the success of the experimental work are greatly appreciated.

REFERENCES

Atkinson, J. D. and Forrest, J. E., 1985, "Factors Influencing the Rate of Growth of Fatigue Cracks in RPV Steels Exposed to a Simulated PWR Primary Water Environment", *Corrosion Science*, Vol. 25, No. 8/9, pp. 607-631.

Combrade, P., Foucault, M. and Slama, G., 1988, "Effect of Sulfur on the Fatigue Crack Growth Rates of Pressure Vessel Steel Exposed to PWR Coolant: Preliminary Model for Prediction of the Transitions Between High and Low Crack Growth Rates", *Proceedings of the Third International Conference, Environmental Degradation of Materials in Nuclear Power Systems - Water Reactors*, G. J. Theus and J. R. Weeks (Eds.), TMS-AIME, pp. 269-276.

Eason, E. D., Andrew, S. P., Warmbrodt, S. B., Nelson, E. E. and Gilman, J. D., 1989, "Analysis of Pressure Vessel Steel Fatigue Tests in Air," *Nuclear Engineering and Design*, Vol. 115, No. 1, pp. 23-30

Gabetta, G. and Caretta, E., 1987, "Corrosion-Potential Measurements Inside and Outside a Growing Crack During Environmental Fatigue Tests at 288°C, with Different Oxygen Contents," *Corrosion Chemistry Within Pits, Crevices and Cracks*, Her Majesty's Stationery Office, London, pp. 287-300

Hartt, W. H., Tennant, J. S. and Hooper, W. C., 1978, "Solution Chemistry Modification Within Corrosion-Fatigue Cracks," *Corrosion-Fatigue Technology*, ASTM STP 642, pp. 5-18

James, L. A. and Poskie, T. J., 1993, "Correlation Between MnS Area Fraction and EAC Behavior," WAPD-T-3012, available from US DOE Office of Scientific Technical Information, P.O. Box 62, Oak Ridge, TN 37831

James, L. A., 1994a, "The Effect of Temperature and Cyclic Frequency Upon Fatigue Crack Growth Behavior of Several Steels in an Elevated Temperature Aqueous Environment," *Journal of Pressure Vessel Technology*, Vol. 116, No. 2, pp. 122-127

James, L. A. and Wilson, W. K., 1994b, "Development of a Surface-Cracked Specimen," *Theoretical and Applied Fracture Mechanics*, Vol. 20 No. 2, pp. 115-121

James, L. A., Wire, G. L. and Cullen, W. H., 1995a, "The Effect of Water Flow Rate Upon the Environmentally-Assisted Cracking Response of a Low-Alloy Steel," *Journal of Pressure Vessel Technology*, Vol. 117, No. 3, pp. 238-244

James, L. A., 1995b, "Ramberg-Osgood Strain-Hardening Characterization of an ASTM A302-B Steel," *ibid.*, Vol. 117, No. 4, pp. 341-345

James, L. A., and Mills, W. J., 1995c, "Fatigue Crack Propagation Behavior of Wrought Alloy 600 and Weld-Deposited EN82H in an Elevated Temperature Aqueous Environment", *Service Experience, Structural Integrity, Severe Accidents, and Erosion in Nuclear and Fossil Plants*, ASME Publication PVP-Vol. 303, pp. 21-36

James, L. A., Lee, H. B. and Wire, G. L., 1997a, "The Effect of Water Flow Rate Upon the Environmentally-Assisted Cracking Response of a Low-Alloy Steel: Experimental Results Plus Modeling," *Journal of Pressure Vessel Technology*, Vol. 119, No. 1

James, L. A., Auten, T. A., Poskie, T. J., and Cullen, W. H., 1997b, "Corrosion-Fatigue Crack Growth in Clad Low-Alloy Steels: Part I, Medium-Sulfur Forging Steel," *ibid.*, in press, (WAPD-T-3095)*

James, L. A., Lee, H. B., Wire, G. L., Novak, S. R., and Cullen, W. H., 1997c, "Corrosion-Fatigue Crack Growth in Clad Low-Alloy Steels: Part II, Water Flow Rate Effects in High-Sulfur Plate Steel," *ibid.*, in press, (WAPD-T-3096)*

James, L. A., 1997d, "Surface-Crack Aspect Ratio Development During Corrosion-Fatigue Crack Growth in Low-Alloy Steels", *Nuclear Engineering and Design*, in press, (WAPD-T-3111)*

Kondo, T., Kikuyama, T., Nakajima, H., Shindo, M. and Nagasaki, R., 1972a, "Corrosion Fatigue of ASTM A-302B Steel in High Temperature Water, the Simulated Nuclear Reactor Environment," *Corrosion Fatigue*, NACE-2, National Association of Corrosion Engineers, pp. 539-556

Kondo, T., Kikuyama, T., Nakajima, H. and Shindo, M., 1972b, "Fatigue of Low-Alloy Steels in Aqueous Environment at Elevated Temperatures," *Mechanical Behavior of Materials, Proceedings International Conference on Mechanical Behavior of Materials*, Vol. 3, The Society of Materials Science, Japan, pp. 319-327

Newman, J. C. and Raju, I. S., 1984, "Stress Intensity Factor Equations for Cracks in Three-Dimensional Finite Bodies Subjected to Tension and Bending Loads," NASA Technical Memorandum 85793

Turnbull, A. and Thomas, J. G. N., 1982, "A Model of Crack Electrochemistry for Steels in the Active State Based on Mass Transport by Diffusion and Ion Migration," *Journal of the Electrochemical Society*, Vol. 129, No. 7, pp. 1412-1422

Turnbull, A., 1983, "A Theoretical Evaluation of the Oxygen Concentration in a Corrosion-Fatigue Crack", *Corrosion-Fatigue: Mechanics, Metallurgy, Electrochemistry, and Engineering*, ASTM STP 801, pp. 351-366

Turnbull, A. and Psaila-Dombrowski, M. 1992, "A Review of Electrochemistry of Relevance to Environment-Assisted Cracking in Light Water Reactors," *Corrosion Science*, Vol. 33, No. 12, pp. 1925-1966

VanDerSluys, W. A. and Emanuelson, R. H., 1993, "Environmental Acceleration of Fatigue Crack Growth in Reactor Pressure Vessel Materials", TR-102796, Vol. 1 & 2, EPRI

Wire, G. L. and Li, Y. Y., 1996, "Initiation of Environmentally-Assisted Cracking in Low-Alloy Steels," *Fatigue and Fracture-1996-Volume I,* ASME Publication PVP-Vol. 323, pp. 269-289

*Available from US DOE Office of Scientific Technical Information, P.O. Box 62, Oak Ridge, TN 37831

Table I

CHEMICAL COMPOSITIONS

Alloy	Heat No.	C	Mn	P	S	Si	Mo	Cu	Ni	Cr	Fe	Ti	Cb+Ta
A302-B+	21478-10	0.20	1.25	0.021	0.026	0.22	0.51	0.22	0.22	0.14	Bal.	-	-
EN82H (GMA)	NX4644DK	0.04	2.99	0.001	0.001	0.06	-	0.02	72.74*	19.81	1.38	0.43	2.53

+ Average of several measurements
*Ni+Co

Table II

Summary of Environmental Ratio Parameters for Surface-Cracked Specimens

Specimen Number	Material	Data Reference	Mean ER over Range of ϕ	d(ER)/d(L) (mm^{-1})	Range of ϕ (degrees)	EAC or non-EAC
SC-15	A302-B	Present Work	2.93	0.244	$0° \le \phi \le 70°$	non-EAC
SC-11	A302-B	James (1997d)	3.41	0.164	$0° \le \phi \le 90°$	non-EAC
SC-9	A302-B	James (1997d)	2.48	0.145	$0° \le \phi \le 90°$	non-EAC
YJ2CS1	A302-B/EN82H	Present Work	3.56	0.084	$30° \le \phi \le 90°$	non-EAC
OU4	A508-2/EN82H	James (1997c)	2.42	-0.051	$30° \le \phi \le 90°$	non-EAC
SC-15	A302-B	Present Work	13.90[a]	11.12[b]	$\phi = 90°$	EAC
SC-11	A302-B	James (1997d)	28.38	2.088	$0° \le \phi \le 70°$	EAC
SC-11	A302-B	James (1997d)	59.73[a]	19.92[b]	$\phi = 90°$	EAC
SC-14	A302-B	James (1997d)	10.51	0.726	$0° \le \phi \le 90°$	EAC[c]

Notes: a) Value at $\phi = 90°$
b) Based on the slope from $\phi = 70°$ to $\phi = 90°$
c) "Milder" case of EAC

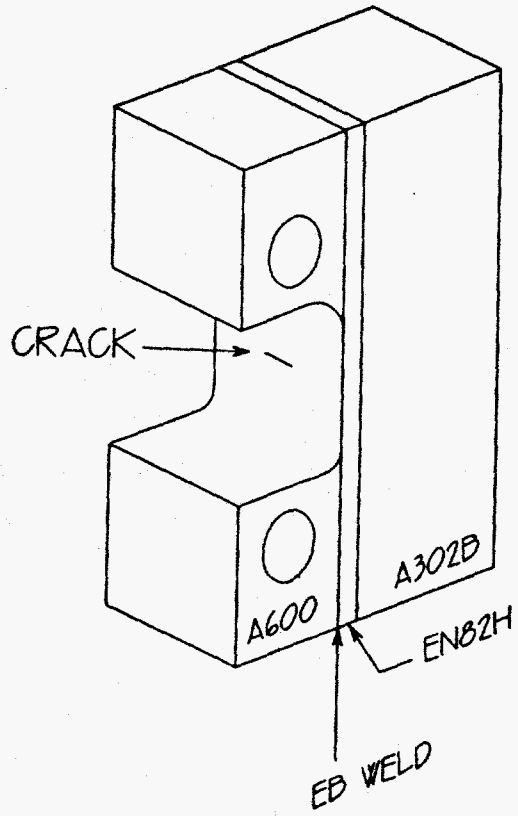

Figure 1. Schematic of the composite A302-B/EN82H/Alloy 600 specimen (Specimen YJ2CS1) with the precracking web removed. The monolithic steel specimen (Specimen SC-15) was similar, but was composed entirely of A302-B steel.

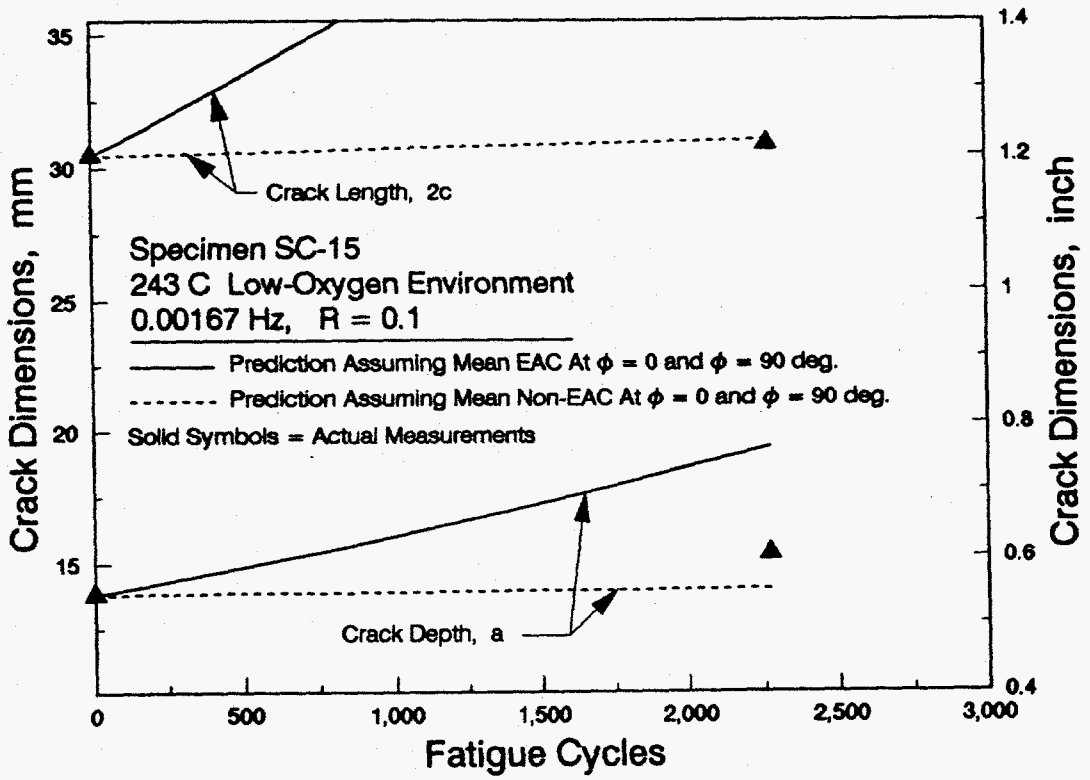

Figure 2. Comparison between the predicted and observed crack extension behavior for the surface-cracked specimen of A302-B steel.

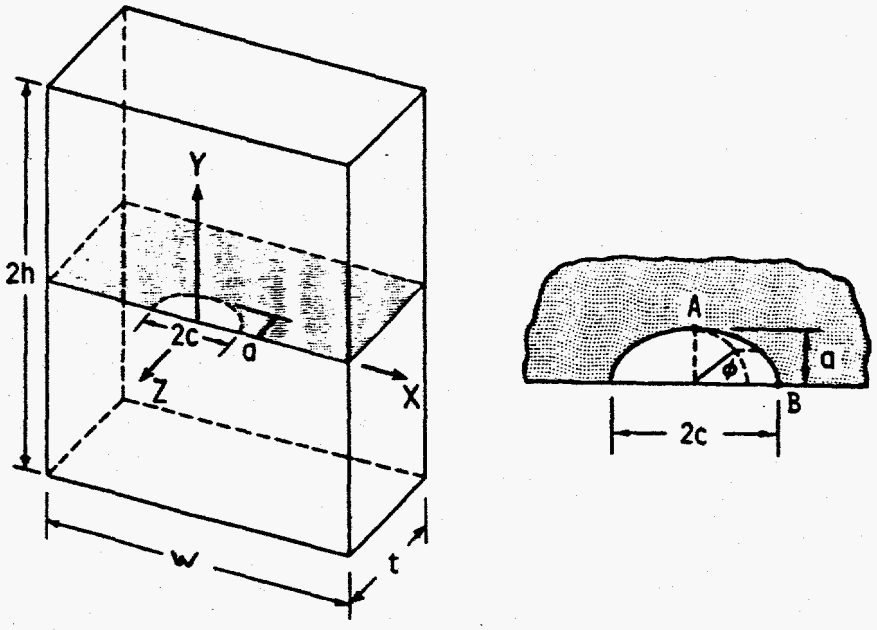

Figure 3. Surface crack in a finite plate. Note the definition of the elliptical angle ϕ

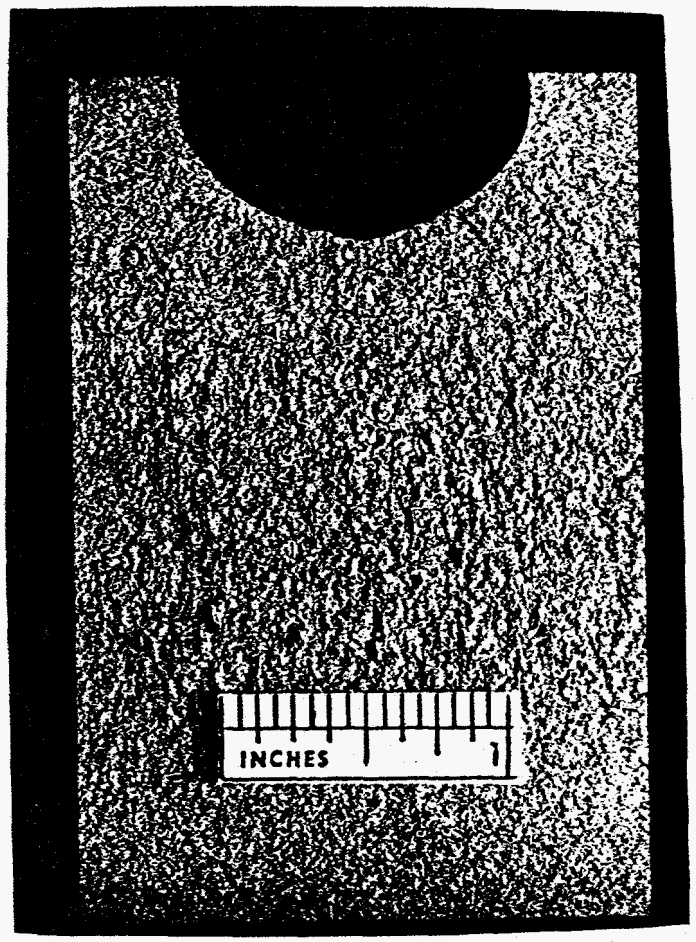

Figure 4. Photomacrograph of the post-test fracture surface for Specimen SC-15. Note the greater amount of crack extension (Δa) at the deepest point (ϕ = 90°) suggesting that EAC had just initiated at that location.

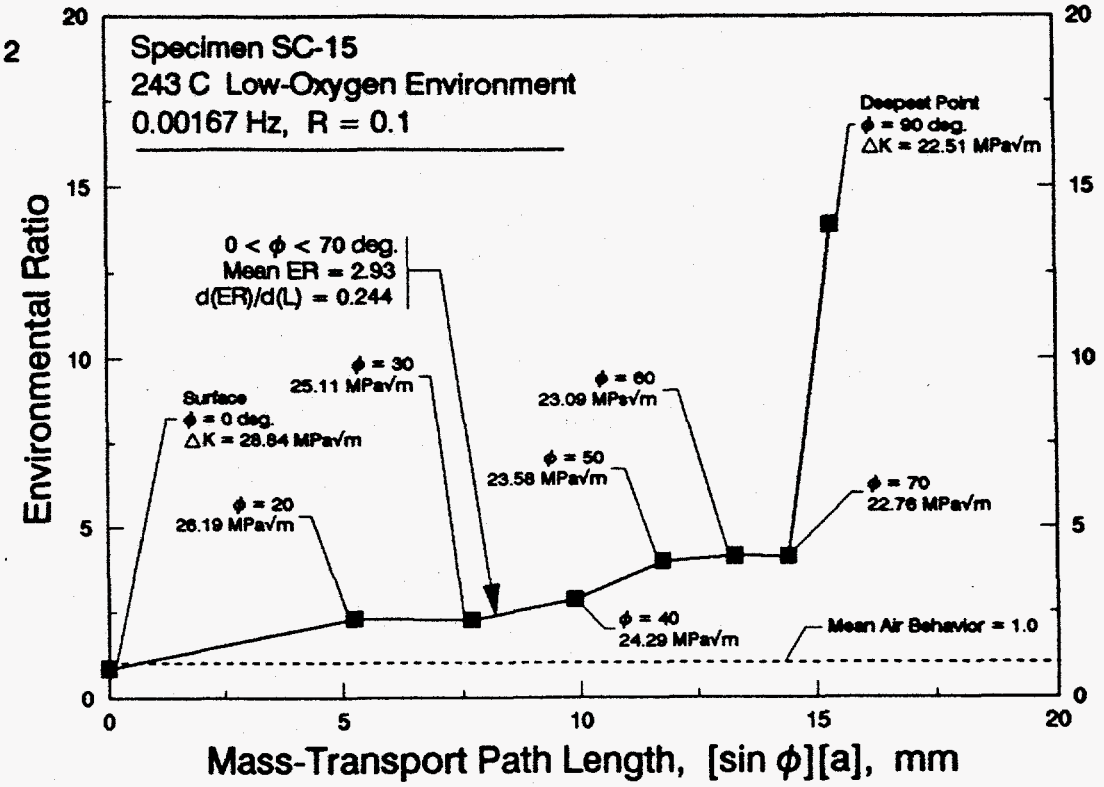

Figure 5. The Environmental Ratio ($å_e/å_b$) as a function of the mass-transport path length. Note the increase in the ER at $\phi > 70°$ representing the initiation of EAC.

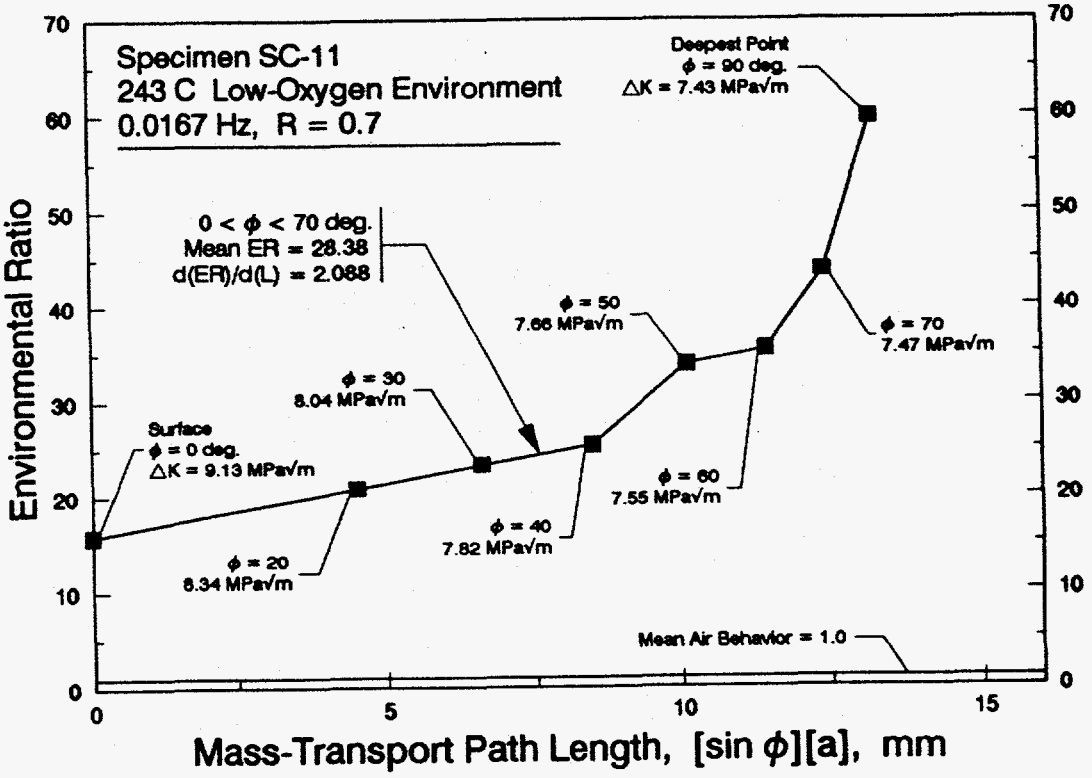

Figure 6. Results of the quasi-stagnant test phase on Specimen SC-11 plotted as the Environmental Ratio as a function of the mass-transport path length. From James (1997d).

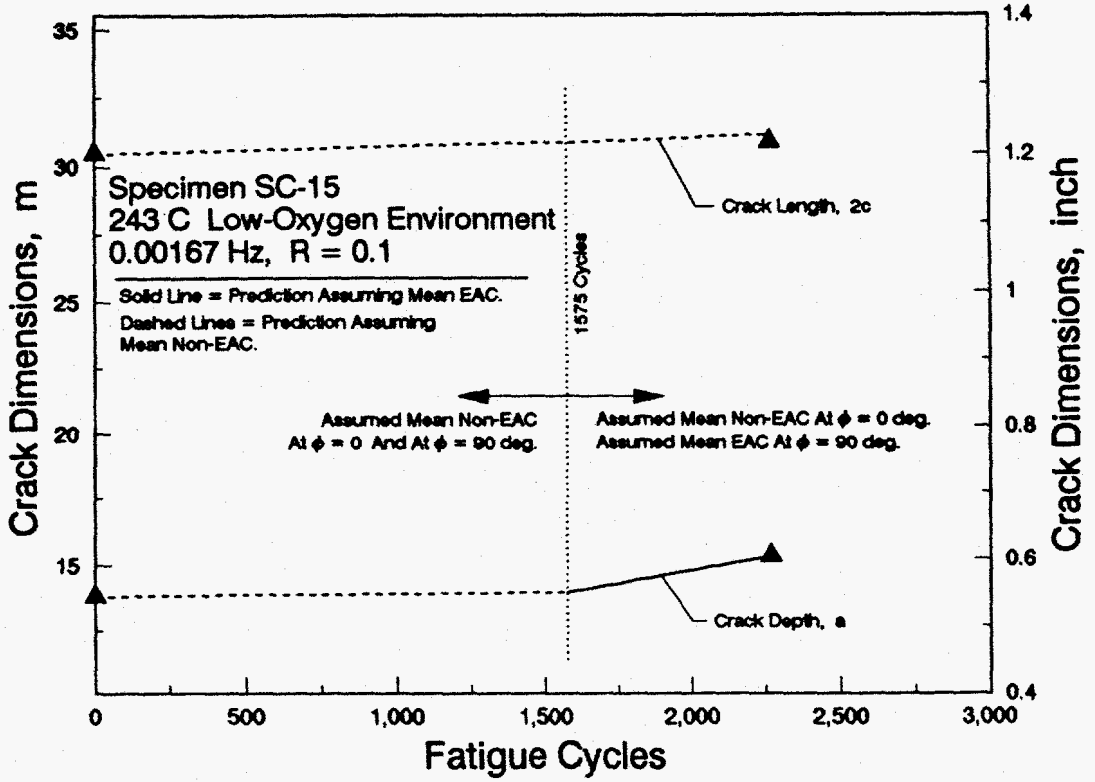

Figure 7. A scenario that would explain the initiation of EAC at $\phi = 90°$ part-way through the experiment on Specimen SC-15.

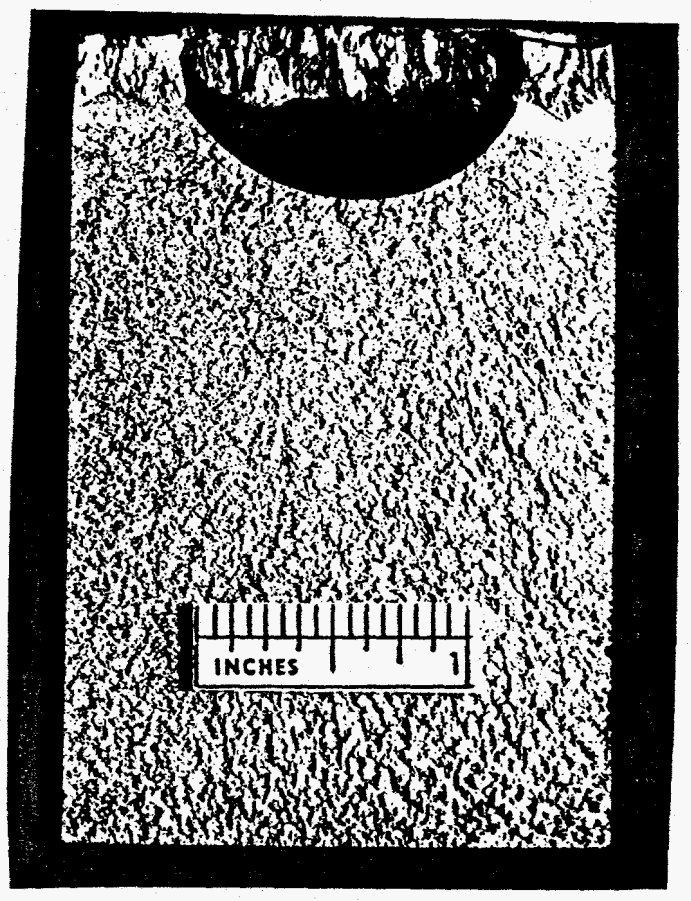

Figure 8. Photomacrograph of the post-test fracture surface for Specimen YJ2CS1. Note the greater crack-surface roughness in the cladding relative to the underlying base metal.

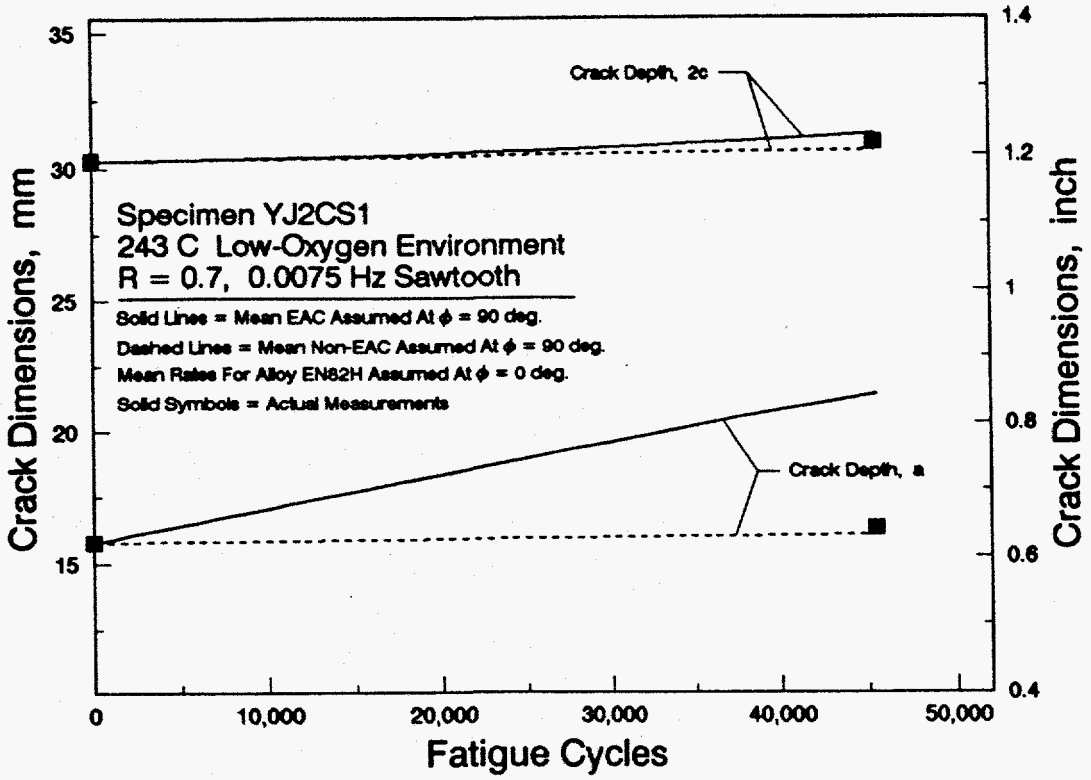

Figure 9. Comparison of the predicted crack extension with the actual pre-test and post-test measurements for Specimen YJ2CS1.

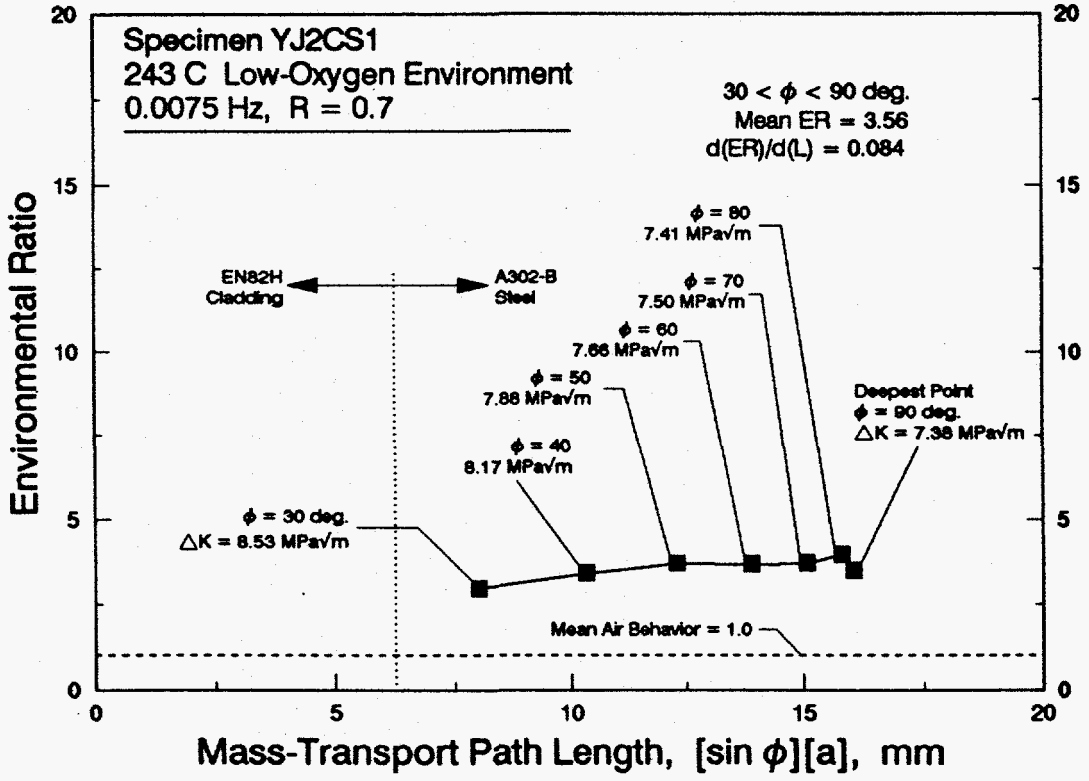

Figure 10. The Environmental Ratio observed at various locations (ϕ = elliptical angle) along the crack front of Specimen YJ2CS1.

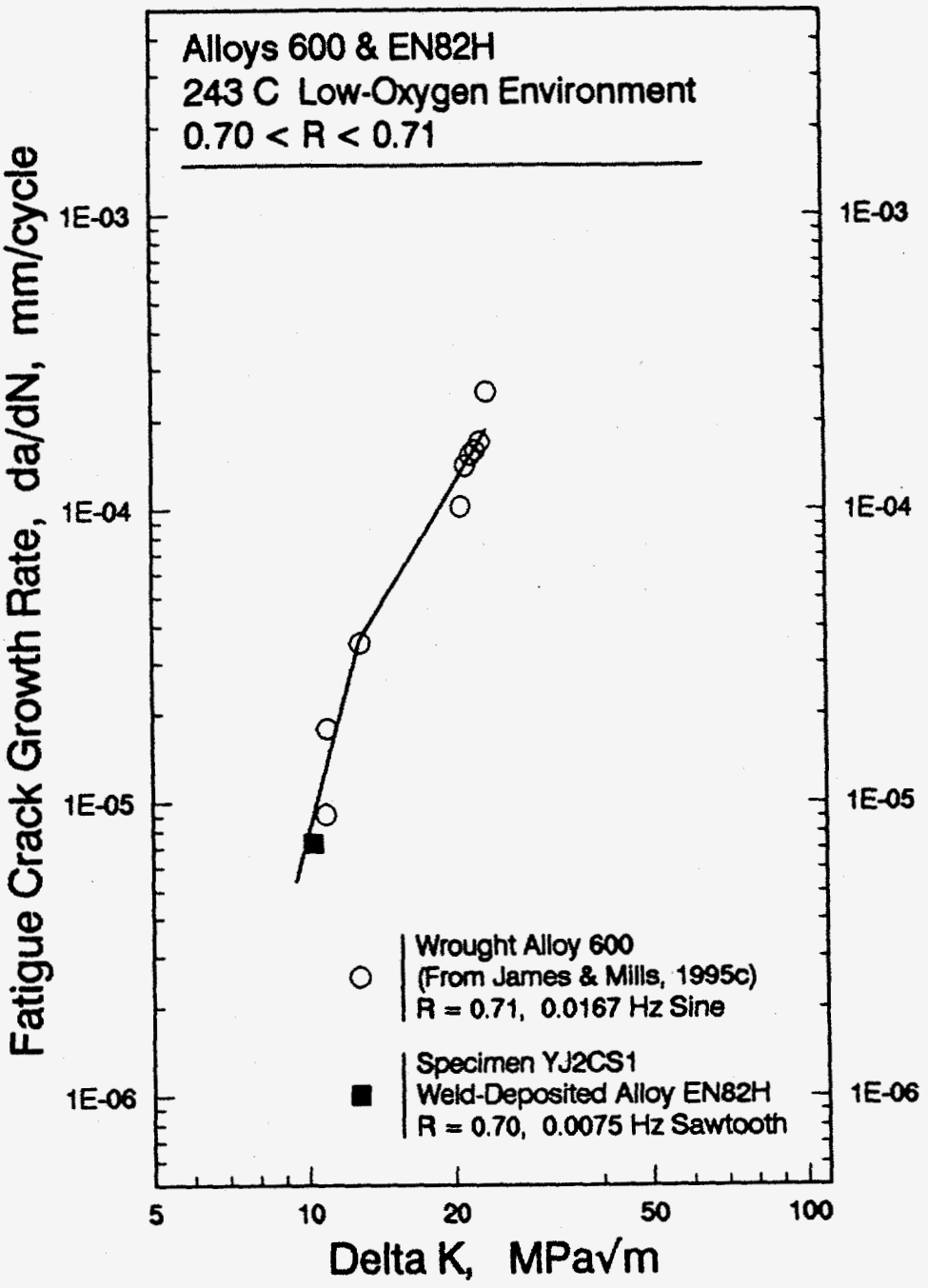

Figure 11. Comparison of the fatigue crack growth behavior of Specimen YJ2CS1 at the surface (EN82H) with that of wrought Alloy 600 tested by James and Mills (1995c) under similar conditions.